

# Synthetic carbon fixation via the autocatalytic serine threonine cycle

Sebastian Wenk\*<sup>1</sup>, Vittorio Rainaldi<sup>1</sup>, Hai He<sup>2</sup>, Karin Schann<sup>1</sup>, Madeleine Bouzon<sup>3</sup>, Volker Döring<sup>3</sup>, Steffen N. Lindner<sup>4</sup>, Arren Bar-Even<sup>1</sup>

<sup>1</sup>Max Planck Institute of Molecular Plant Physiology, Am Mühlenberg 1, 14476 Potsdam-Golm, Germany;

<sup>2</sup>Max Planck Institute of Terrestrial Microbiology, Karl-von-Frisch-Str. 10, 35043 Marburg, Germany

<sup>3</sup>Génomique Métabolique, Genoscope, Institut François Jacob, CEA, CNRS, Univ Evry, Université Paris-Saclay-4, 91057 Evry-Courcouronnes, France.

<sup>4</sup>Department of Biochemistry, Charité Universitätsmedizin, Virchowweg 6, 10117 Berlin, Germany

\*Corresponding author. Phone: +49 331 5678254. Email: [wenk@mpimp-golm.mpg.de](mailto:wenk@mpimp-golm.mpg.de)

## Abstract

Atmospheric CO<sub>2</sub> poses a major threat to life on Earth by causing global warming and climate change. On the other hand, it is the only carbon source that is scalable enough to establish a circular carbon economy. Accordingly, technologies to capture and convert CO<sub>2</sub> to reduced one-carbon (C<sub>1</sub>) molecules (e.g. formate) using renewable energy are improving fast. Driven by the idea of creating sustainable bioproduction platforms, natural and synthetic C<sub>1</sub>-utilization pathways are engineered into industrially relevant microbes. The realization of synthetic C<sub>1</sub>-assimilation cycles in living organisms is a promising but challenging endeavour. Here, we engineer the autocatalytic serine threonine cycle, a synthetic C<sub>1</sub>-assimilation route in *Escherichia coli*. Our stepwise engineering approach in tailored selection strains combined with adaptive laboratory evolution experiments enabled the organism to grow on formate. The synthetic strain uses formate as the sole carbon and energy source and is capable of growing at ambient CO<sub>2</sub> concentrations, demonstrating the feasibility of establishing synthetic C<sub>1</sub>-assimilation cycles over laboratory timescales.

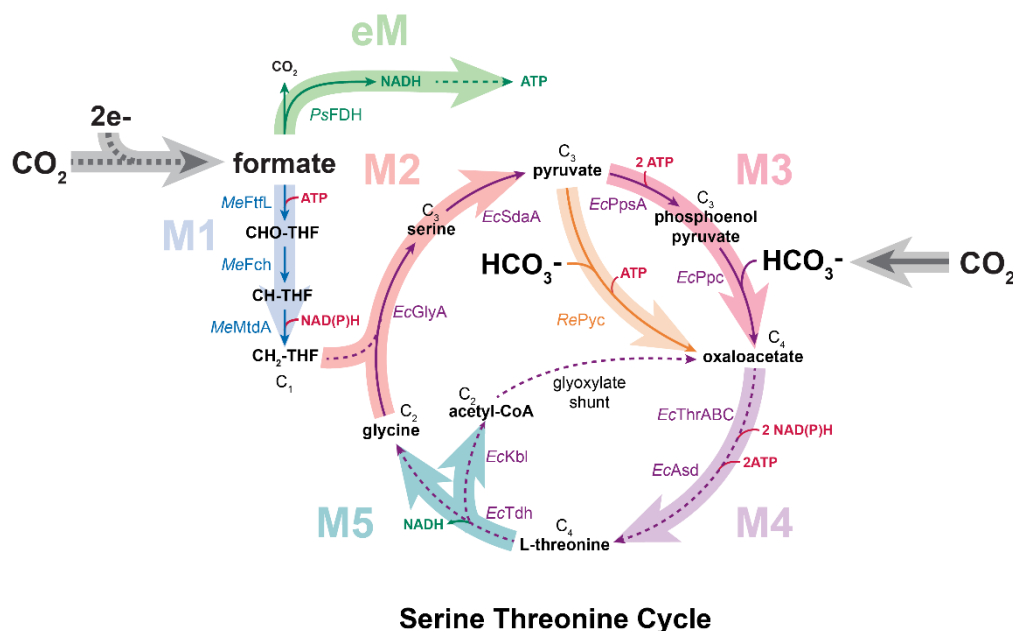
## Introduction

The transition from a fossil-based, CO<sub>2</sub>-emitting economy towards a circular CO<sub>2</sub>-neutral economy is an imminent challenge to avert climate catastrophes<sup>1</sup>. CO<sub>2</sub> is threatening our way of life by causing climate change and global warming, but, at the same time it is the only feedstock scalable enough to provide carbon for chemical or microbial production processes. Chemistry offers several efficient options to reduce CO<sub>2</sub> into simple one-carbon (C<sub>1</sub>) molecules like formate or methanol, however, multi-carbon molecules cannot be produced with a high productivity<sup>2,3</sup>. Here, microbial cell factories can fill the gap to produce more complex value-added chemicals. Driven by this concept, industrially relevant model microbes have been engineered to grow on C<sub>1</sub> molecules as sole carbon sources<sup>4-8</sup>. Formate has been determined a key C<sub>1</sub> molecule, as it can be produced very efficiently from CO<sub>2</sub> and presents similar physicochemical properties to methanol<sup>9-12</sup>. In nature, formate serves as a carbon and energy source to organisms growing via the serine cycle, the reductive glycine pathway (rGlyP) and the Calvin–Benson–Bassham (CBB) cycle (aerobic growth) or the reductive acetyl-CoA pathway (anaerobic growth)<sup>2,13-16</sup>. To facilitate the engineering of formatotrophy in industrially relevant microbes, several synthetic formate assimilation pathways were suggested and characterized computationally<sup>2,17,18</sup>. Among them, the serine threonine cycle (STC) was described as highly suitable for implementation in model microbes like *E. coli* and for biotechnological applications (Figure 1). It is oxygen tolerant, operates at ambient CO<sub>2</sub> concentrations, requires the expression of only a few foreign enzymes and since it is an autocatalytic cycle, it has the potential to support exponential growth<sup>19</sup>. Autocatalytic cycles are very common in nature due to their optimal network topology but are considered difficult to engineer as they are susceptible to instabilities<sup>20</sup>. The design of the STC resembles the structure of the natural serine cycle (Supplementary Figure 1)<sup>13</sup>, but is modified to rely on the endogenous metabolism of *E. coli* for most of the pathway reactions<sup>17</sup>.

The implementation of the long and complex cycle in the heart of *E. coli*'s metabolism (the STC overlaps with glycolysis and the highly regulated PEP–pyruvate–oxaloacetate node<sup>21</sup>) requires a substantial rerouting of central metabolic fluxes and is expected to reveal fundamental insights into the plasticity of the central metabolic network. In recent years, several studies enabled C<sub>1</sub>-dependent growth of *E. coli* via natural autocatalytic cycles, overlapping with the pentose phosphate pathway and glycolysis: autotrophic growth via the CBB cycle<sup>4</sup> and methylotrophic growth via the ribulose monophosphate (RuMP) cycle<sup>6,22</sup>. Also, very recently a synthetic autocatalytic cycle for CO<sub>2</sub> fixation was demonstrated

55 in the strict anaerobe *Clostridium ljungdahlii*<sup>23</sup>. For formatotrophic growth, the non-autocatalytic, linear rGlyP has been  
 56 established in *E. coli*<sup>5</sup>, but previous attempts to establish a natural autocatalytic formate assimilation cycle<sup>24</sup> or a  
 57 synthetic formaldehyde assimilation cycle<sup>25</sup> required the addition of co-substrates and so far, cyclic pathway activity was  
 58 not reported. Thus, the engineering of the autocatalytic, new-to-nature STC in *E. coli* would overcome an open challenge  
 59 to synthetic biology.

60 Here, we report the establishment of the complete STC and the conversion of the obligate heterotroph *E. coli* to a full  
 61 formatotroph. We show that a combination of targeted engineering and adaptive laboratory evolution (ALE) enables the  
 62 activity of the complete cycle. First, we engineered auxotrophic strains that depended on pathway activity for growth<sup>26</sup>.  
 63 Then, we expressed individual pathway modules to complement the strain's auxotrophies. Finally, we used ALE to  
 64 overcome metabolic bottlenecks that prevented cyclic pathway activity achieving formatotrophic growth via the STC  
 65 within ~200 days of evolution. After confirming the formatotrophic phenotype of isolated strains by growth and isotopic  
 66 labelling experiments, we analysed genomic alterations via genome sequencing and determined a small number of  
 67 mutations that enabled activity of the STC. This study shows for the first time a fully functional autocatalytic and new-  
 68 to-nature C<sub>1</sub>-assimilation cycle in *E. coli*, which enables the organism to grow on the sustainable C<sub>1</sub>-substrate formate  
 69 at ambient CO<sub>2</sub> concentration.



**Serine Threonine Cycle**

**Figure 1: The autocatalytic serine threonine cycle is suited for synthetic carbon fixation in *E. coli*.**

71 To run the synthetic cycle in *E. coli*, most of the reactions can be catalyzed by endogenous enzymes (purple arrows). CO<sub>2</sub>-derived  
 72 formate is converted into the one-carbon (C<sub>1</sub>) molecule methylene-THF (CH<sub>2</sub>-THF) via module 1 (M1) of the STC. The carbon from  
 73 CH<sub>2</sub>-THF is attached to glycine producing the three-carbon (C<sub>3</sub>) molecule serine which is converted to pyruvate (M2). In M3 (the four-  
 74 carbon (C<sub>4</sub>) molecule), pyruvate is converted to oxaloacetate fixing CO<sub>2</sub> in the form of HCO<sub>3</sub><sup>-</sup> either via phosphoenolpyruvate (PEP)  
 75 carboxylation (red arrow) or direct carboxylation of pyruvate (orange arrow). From oxaloacetate, threonine is produced (M4) and then  
 76 cleaved into the two-carbon (C<sub>2</sub>) molecules glycine and acetyl-CoA (M5). As acetyl-CoA can be converted into oxaloacetate via the  
 77 glyoxylate shunt, the cycle becomes autocatalytic. An energy module (eM) consisting of a NAD-dependent formate dehydrogenase  
 78 supplies the cell with reduction equivalents and ATP derived from formate. CO<sub>2</sub> reduction to formate is achieved electrochemically  
 79 (grey dotted arrow). *Ps*, *Pseudomonas sp. (strain 101)*; *Me*, *Methylorubrum extorquens*; *Ec*, *Escherichia coli*; *Re*, *Rhizobium etli*;  
 80 THF, tetrahydrofolate; Fdh, formate dehydrogenase; FtlL, formate-THF ligase; Fch, methenyl-THF cyclohydrolase; MtdA, methylene-  
 81 THF dehydrogenase; GlyA, serine hydroxymethyltransferase; SdaA, serine deaminase; PpsA, PEP synthetase; Ppc, PEP  
 82 carboxylase; Pyc, pyruvate carboxylase; ThrA, aspartate kinase I / homoserine dehydrogenase I; ThrB, homoserine kinase; ThrC,  
 83 threonine synthase; Asd, aspartate-semialdehyde dehydrogenase; Tdh, threonine dehydrogenase and Kbl, 2-amino-3-ketobutyrate  
 84 CoA ligase.

## 86 Results

### 87 Pathway modularization enables the stepwise engineering of the STC

88 To facilitate the engineering of the STC in *E. coli*, we divided the pathway into six metabolic modules (M) (Figure 1) that  
89 could be tested individually or in combination in dedicated selection strains: (M1) the C<sub>1</sub> module that converts CO<sub>2</sub>-  
90 derived formate into CH<sub>2</sub>-THF; (M2) the C<sub>3</sub> module that converts CH<sub>2</sub>-THF and glycine into pyruvate; (M3) the C<sub>4</sub> module  
91 that converts pyruvate into oxaloacetate; (M4) the threonine synthesis module that drives the carbon flux from  
92 oxaloacetate towards threonine; (M5) the threonine cleavage module that cleaves threonine into glycine and acetyl-CoA  
93 and (eM) the energy module that oxidizes formate to generate NADH<sup>27</sup>. Module enzymes that are not naturally encoded  
94 in the *E. coli* genome were cloned into synthetic operons using defined promoters and ribosome binding sites (RBS) to  
95 modulate their expression levels and were expressed from the genome. Native *E. coli* enzymes were overexpressed  
96 when necessary by a genomic promoter exchange. Modules were tested for their *in vivo* activity in dedicated selection  
97 strains that depend on module activity for cell growth.

### 99 Rewiring *E. coli*'s central metabolism for the implementation of the STC

100 As a substantial rewiring of *E. coli*'s central metabolism is required for the implementation of the STC - the main carbon  
101 flux needs to be directed from oxaloacetate to threonine (M4) which is cleaved to produce glycine and acetyl-CoA  
102 (M5)<sup>17</sup> - we first created a selection strain that depends on the combined activity of M4 and M5 for cell growth (hereafter  
103 referred to as XGAS). This strain is practically auxotrophic to acetyl-CoA, serine and glycine as the canonical routes to  
104 these metabolites are blocked through gene deletions (Figure 2A). XGAS is only able to grow on glycerol if both M4 and  
105 M5 are sufficiently active to divert a major fraction of the cellular carbon flux via threonine synthesis and cleavage. When  
106 cultivated on glycerol, the strain was not able to grow, indicating that endogenous expression of M4 and M5 genes does  
107 not support sufficient flux towards acetyl-CoA and glycine. Only when the threonine cleavage module M5 was  
108 overexpressed from the genome (XGAS:gM5), growth on glycerol was observed (Figure 2B). Additional overexpression  
109 of M4 did not improve growth on glycerol, indicating that the creation of a strong sink for threonine through the expression  
110 of M5 also increased the flux towards its synthesis. We thus continued the engineering of the STC with the XGAS:gM5.  
111 In the next step, we included the formate assimilation module M1 into the pathway selection. To test for its activity, we  
112 deleted the glycine cleavage system (GCS) in the XGAS:gM5 strain, creating XGAS\_C1:gM5. The GCS deletion  
113 prevents glycine cleavage into CH<sub>2</sub>-THF and CO<sub>2</sub>. Thus, XGAS\_C1:gM5 is auxotrophic to metabolites derived from  
114 CH<sub>2</sub>-THF (e.g. methionine, purines, CoA and thymidine) and cannot produce serine from glycine. Expression of the  
115 enzymes of the C<sub>1</sub>-module (M1) in the XGAS\_C1:gM5 strain establishes formate as the precursor of the essential THF-  
116 bound C<sub>1</sub> moieties. As previous studies determined M1 enzymes from *Methylobacterium extorquens* suitable for formate  
117 assimilation in *E. coli*<sup>5,28</sup>, these genes were cloned into a synthetic operon and integrated into the genome of  
118 XGAS\_C1:gM5. Upon integration of M1, the strain was able to grow on glycerol when formate was supplied as a co-  
119 substrate (Figure 2D).

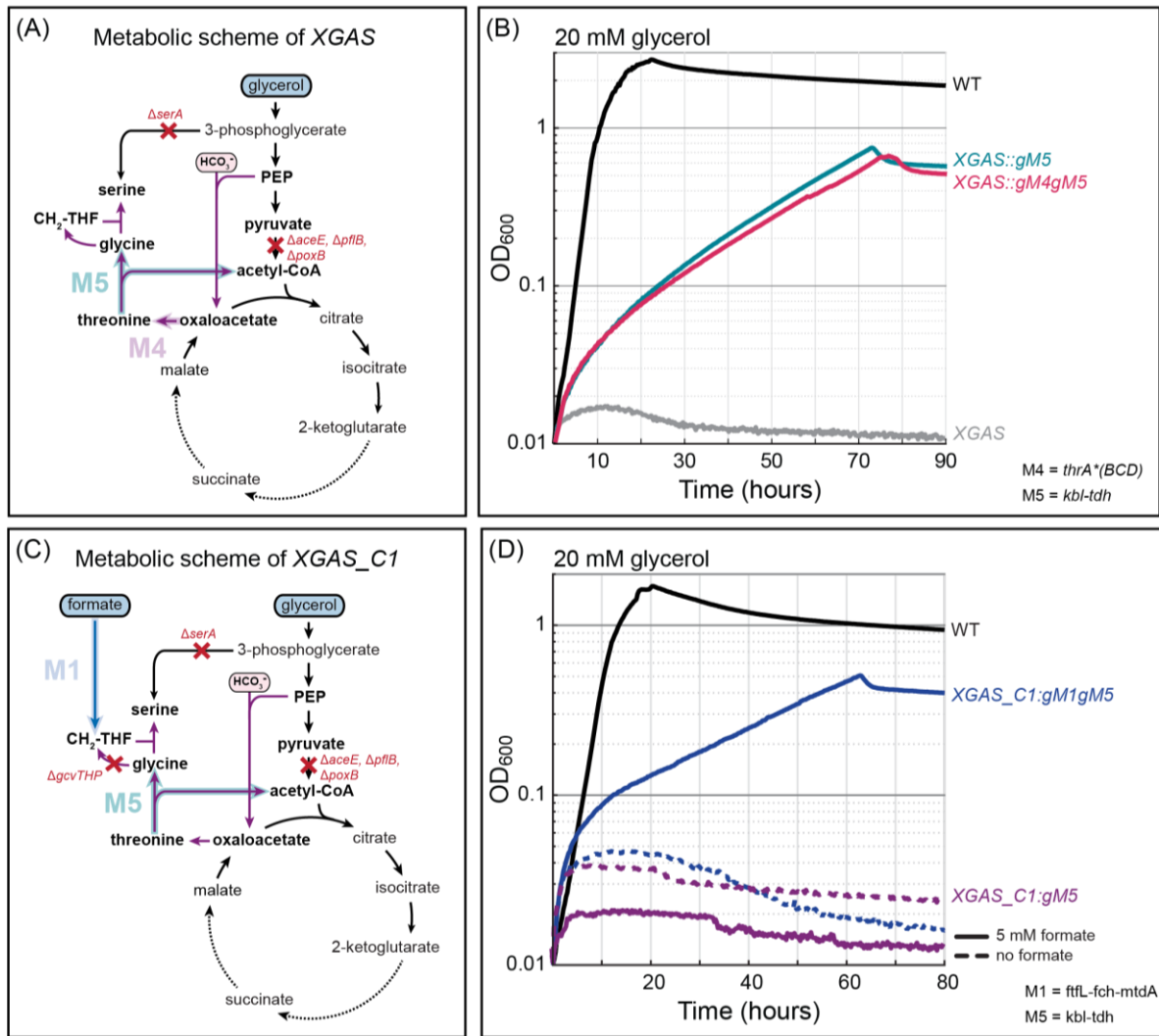


**Figure 2: Rerouting of central metabolic fluxes enables growth via STC modules 1, 4 and 5.**

(A) Metabolic scheme of the XGAS selection strain that can only grow if modules 4 and 5 of the STC are sufficiently active to produce all cellular acetyl-CoA and glycine from threonine. (B) Overexpression of M5 from the genome (gM5) enabled the strain to grow on glycerol. Growth was not improved when also M4 was overexpressed from the genome. (C) Selection scheme of the strain XGAS\_C1 which cannot produce serine from glycine as the glycine cleavage system genes (*gcvTHP*) are deleted. The auxotrophy can only be released if formate is assimilated into CH<sub>2</sub>-THF by M1 enzymes. (D) When both M1 and M5 of the STC were expressed from the genome and formate was provided in the medium the strain was able to grow. Growth experiments were performed within 96-well plates in triplicates, which resulted in identical curves ( $\pm 5\%$ ), and hence were averaged. All experiments (in triplicates) were repeated three times, which showed highly similar growth behavior. WT, wild type; *serA*, phosphoglycerate dehydrogenase; *aceE*, pyruvate dehydrogenase; *poxB*, pyruvate oxidase and *pfkB*, pyruvate formate lyase.

## Optimization of pathway energetics and adaptive laboratory evolution enable cyclic pathway activity

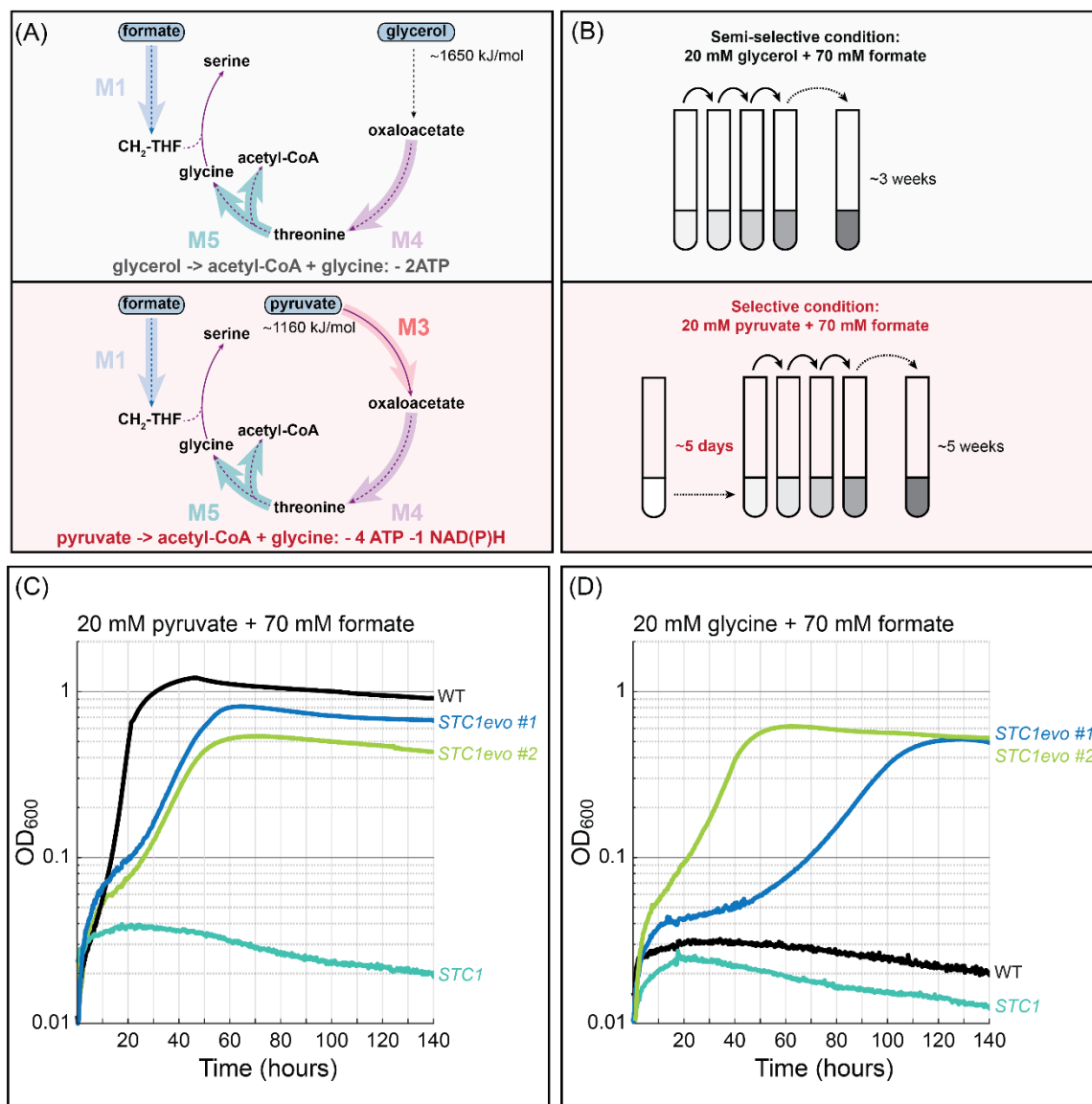
The strain XGAS\_C1:gM1gM5 was able to grow on glycerol and formate via M1, M4 and M5 of the STC but could not grow on pyruvate and formate which also selects for the complete activity of M3 and is an important step towards complete STC activity (Supplementary Figure 2). The reason for that might be related to pathway energetics: the net energy investment for the conversion of pyruvate to acetyl-CoA and glycine via the STC (4 ATP and 1 NAD(P)H) is much higher compared to glycerol (2 ATP) while pyruvate is more oxidized than glycerol (energy of combustion of pyruvate  $\sim 1160$  kJ/mol and glycerol  $\sim 1650$  kJ/mol<sup>29</sup>) (Figure 3A). Hence, it is likely that the cell cannot derive sufficient energy from pyruvate to run the pathway reactions.

To improve pathway energetics, we considered a pyruvate carboxylase (*Pyc*) as an alternative M3 and expression of the eM. The direct carboxylation of pyruvate to oxaloacetate shortens the STC by one reaction and reduces its ATP requirement by one ATP while the FDH of the eM supplies NADH from formate. After verifying *Pyc* activity *in vivo* (Supplementary Figure 3), we integrated *pyc* and the *fdh* into the genome of XGAS\_C1:gM1gM5. As this strain was still not able to grow on pyruvate and formate, we concluded that other metabolic bottlenecks might exist that cannot be easily determined and addressed by rational engineering. Hence, we decided to use short-term ALE in tubes (ALE1) to enable sufficient pathway activity and achieve growth on pyruvate and formate (Figure 3B). We further engineered the



148  
149  
150  
151  
152  
153  
154  
155

strain to express M2 from the genome and conducted the ALE experiment as described in the methods section. After app. 9 weeks, we isolated single colonies capable of growing efficiently on pyruvate and formate via M1, M3, M4 and M5 of the STC (Figure 3C). Surprisingly, when testing the evolved strains with different carbon sources, we found that they were also able to grow on glycine and formate (Figure 3D). This indicated for the first time cyclic pathway activity of the STC and suggests that all modules are active *in vivo*: formate is assimilated into CH<sub>2</sub>-THF which is attached to glycine to form serine (M1 and M2). Then, serine is metabolized via the complete STC to produce acetyl-CoA required for cell growth (M3, M4 and M5).



156  
157  
158  
159  
160  
161  
162  
163  
164  
165  
166  
167  
168  
169

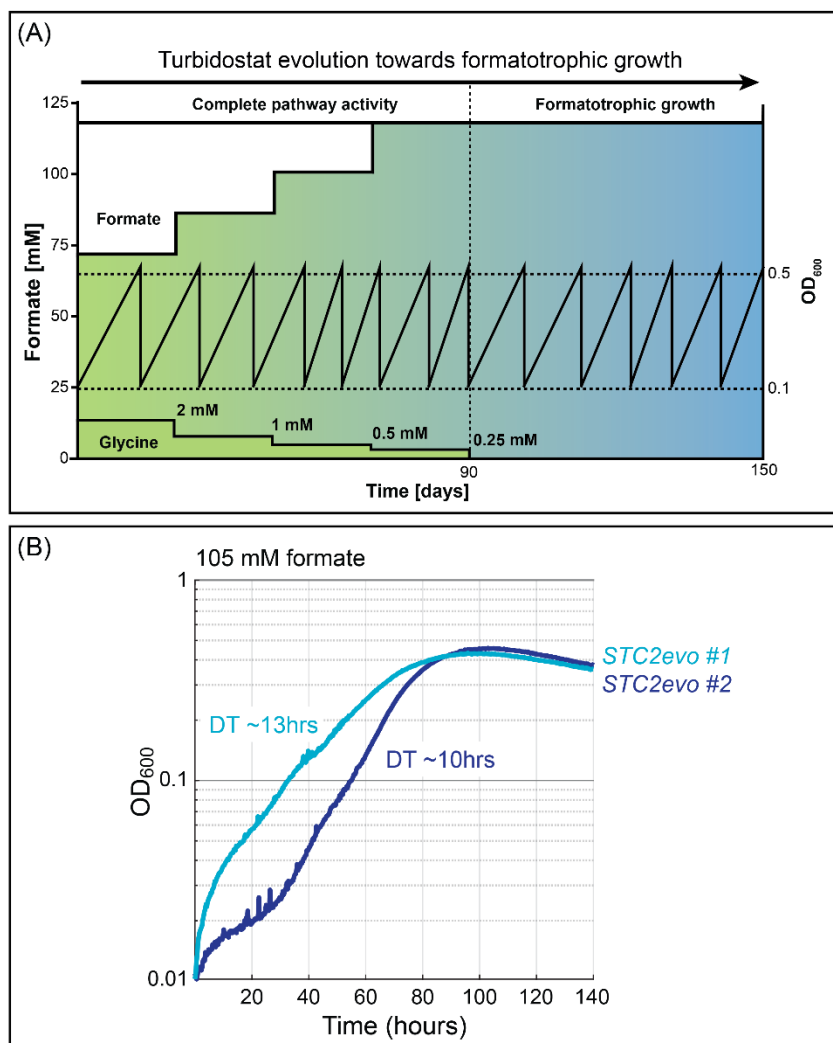
**Figure 3: Strain optimization and adaptive laboratory evolution enable cyclic pathway activity (ALE1).**

(A) The conversion of pyruvate into acetyl-CoA and glycine via the STC requires the combined activity of M1, M3, M4 and M5. Furthermore, it requires the investment of additional two ATPs and one NAD(P)H compared to glycerol. This energetic difference might explain why *XGAS\_C1:gM1gM5* was not able to grow on pyruvate and formate. (B) To achieve growth on pyruvate and formate, the a further engineered strain (*XGAS\_C1:gM1gM2gM3gM5geM* (*STC1*)) was continuously cultivated in tubes with 20 mM glycerol and 70 mM formate for ~3 weeks thereby adapting the strain to high formate concentrations. Whenever the culture reached an OD<sub>600</sub> > 0.5 it was diluted into fresh medium to an OD<sub>600</sub> ~0.01. After ~3 weeks the medium was exchanged to fully selective medium containing 20 mM pyruvate and 70 mM formate. Approximately 5 days after the medium change the culture started to grow. Cultivation in selective medium was continued for ~5 weeks, then single colonies were isolated. (C) Isolated *STC1evo* strains were able to grow on pyruvate and formate and could also grow on (D) glycine and formate suggesting a fully active STC for the production of acetyl-CoA. Growth experiments were performed within 96-well plates in triplicates, which resulted in identical curves ( $\pm 5\%$ ), and hence were averaged. All experiments (in triplicates) were repeated three times, which showed highly similar growth behavior. Abbreviations as in Figure 1.

170  
171  
172  
173  
174  
175  
176  
177  
178  
179  
180  
181  
182

## Developing formatotrophic growth via the STC

As complete activity of the STC was demonstrated for growth on glycine and formate, we aimed to achieve full formatotrophic growth via the pathway in the next step. This however requires at least a 1.63-fold increase in formate uptake (estimated by FBA; see Supplementary Figure 4 and methods) resulting in higher fluxes through the cycle and the energy module. As the strain *STC2* (an *STC1evo* strain with integrated *aceAB* operon) was not able to grow on formate only, we decided to evolve it in an automated setup (Chi.Bio)<sup>30</sup> under turbidostat conditions (ALE2), where glycine was provided as a limiting surrogate substrate which was stepwise decreased while the formate concentration was increased (Figure 4A). Starting from day ~90, we completely omitted glycine in the growth medium. The sustained growth with formate as the sole carbon and energy source suggested the emergence and take-over of a glycine-independent strain that could grow formatotrophic. The cultivation with formate was continued for ~60 days to improve the growth rate of the culture. Then, individual colonies were isolated and their formatotrophic growth was validated. The isolated evolved strains (*STC2evo* #1 and #2) grew robustly on formate without addition of another carbon source indicating that the STC was fully active (Figure 4B).



183  
184  
185  
186  
187  
188  
189  
190  
191  
192  
193

**Figure 4: Automated adaptive laboratory evolution enables formatotrophic growth via the STC (ALE2).**

(A) Schematic of the automated adaptive laboratory evolution setup: In a Chi.Bio reactor the *STC1evo+* strain capable of growing on glycine and formate was continuously cultivated in a turbidostat mode keeping the culture in exponential phase (whenever the OD<sub>600</sub> crossed the threshold of OD<sub>600</sub> 0.5, the culture was diluted to OD<sub>600</sub> 0.1 with fresh medium). Starting with a medium composition of 2 mM glycine and 70 mM formate, over the course of the experiment the glycine concentration was stepwise reduced to 0 mM while the formate concentration was increased to 120 mM. From day ~90 onwards, the culture started to grow fully formatotrophic. (B) Two isolated strains grew on formate only. Growth experiments were performed within 96-well plates in triplicates, which resulted in identical curves ( $\pm 5\%$ ), and hence were averaged. All experiments (in triplicates) were repeated three times, which showed highly similar growth behavior. Doubling times (DT) are indicated in the figure.

## <sup>13</sup>C isotopic labelling confirms formatotrophic growth via the STC

To confirm the incorporation of formate into *E. coli* metabolism, we performed a comprehensive isotopic labelling experiment. To this end, we cultivated the formatotrophic strain *STC2evo* on minimal medium supplemented with 105 mM <sup>13</sup>C-formate and analysed the carbon labelling of proteinogenic amino acids. Feeding with <sup>13</sup>C-formate should lead to incorporation of <sup>13</sup>C into proteinogenic amino acids which can be detected by liquid chromatography–mass spectrometry (LC-MS). As expected, all pathway-related amino acids were labelled confirming their origin in formate and providing definitive evidence for the activity of the STC (Figure 5 and Supplementary Figure 5). The fact that some amino acids were not completely labelled can be explained by the incorporation of unlabelled HCO<sub>3</sub><sup>-</sup> via M3 of the STC (based on the labelling pattern of proline and arginine, we estimated ~25% of intracellular CO<sub>2</sub> to be unlabelled<sup>4</sup>) and the unlabelled fraction of the <sup>13</sup>C-formate (99% pure).

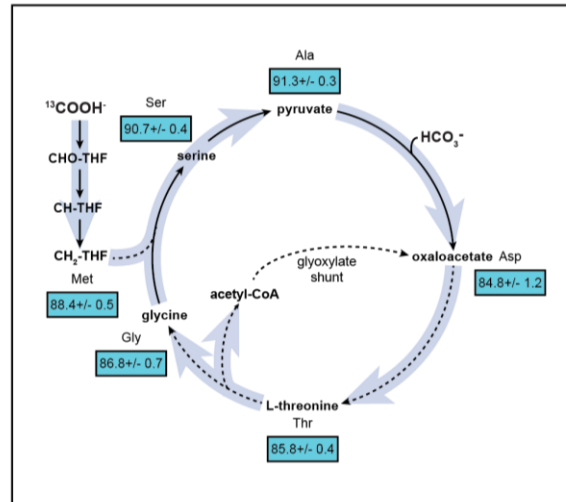


**Figure 5: Incorporation of <sup>13</sup>C-labelled formate confirms formatotrophic growth via the STC.**

The *STC2evo* strain capable of growing on formate was cultivated with 105 mM <sup>13</sup>C-formate and its incorporation into proteinogenic amino acids was analysed via liquid chromatography–mass spectrometry. The analysis showed almost complete labelling of all proteinogenic amino acids. The numbers in the boxes represent the average total carbon labelling of the respective amino acid including standard deviation. The unlabelled fraction of amino acids is derived from unlabelled HCO<sub>3</sub><sup>-</sup> assimilated via M3 of the STC. The experiment (in triplicates) was repeated three times and showed highly similar results.

## A small set of mutations enables formatotrophic growth via the STC

To elucidate the genetic adaptations that enabled cyclic pathway activity we sent genomic DNA of several candidate strains for genome sequencing. Apart from mutations that arose in individual strains and thus cannot be easily attributed to the pathway activity (Supplementary Table 2), all strains carried the same 39bp deletion between the leader peptide of the threonine biosynthesis operon (*thrL*) and the first gene of the operon (*thrA*) (Supplementary Figure 6). Analysing this genomic region in detail, we discovered that the deletion removes an RNA stem loop important for induction of attenuation in the presence of high intracellular threonine concentrations<sup>31</sup>. We assume that the 39bp deletion abolishes attenuation and enables constitutive expression of the of the *thrABC* operon even at elevated threonine levels occurring during growth via the STC. This hypothesis is supported by the fact that growth via the complete STC was abolished when we reconstituted the WT *thrLABC* operon in an evolved strain (Supplementary Figure 6). In addition to the 39bp deletion (which arose during ALE1), the formatotrophic strains incorporated a point mutation in the threonine biosynthesis gene *thrA* leading to a distinct amino acid exchange in the enzyme's regulatory domain (S310P or S440P) which might influence the feedback inhibition of ThrA by threonine. Another mutation observed in all sequenced formatotrophic strains is a single base-pair substitution in the promoter region of the membrane-bound transhydrogenase (*pntAB*) that catalyses the proton transfer from NADH to NADP<sup>+</sup>. Surprisingly, the same mutation was found in a previous study where *E. coli* was engineered to grow on formate via the rGlyP<sup>5</sup>. In this study, quantitative PCR determined that the mutation increases transcript levels of *pntAB* by 13-fold. The higher expression of the transhydrogenase could have a beneficial effect on NADPH availability, a key cofactor for the activity of the STC. While several other mutations were observed in the different evolved strains, the fact that they are not shared among all strains suggests that they are not strictly needed for optimized pathway activity. Hence it seems that a small number of mutations that influences expression and activity of M4 as well as pathway energetics is responsible for the activation of the STC in the engineered strains.

## Discussion

In this study, a new-to-nature autocatalytic formate assimilation cycle in a model microbe has been established. Using a strategy that couples pathway activity to the growth of the host organism combined with ALE, we showed that it is possible to convert the obligate heterotrophic organism *E. coli* into a full formatotroph over laboratory timescales. Our findings are in line with recent studies that successfully established natural C<sub>1</sub> assimilation pathways in *E. coli* (CBB, rGlyP and RuMP) by similar strategies<sup>4-6,22</sup>.

Compared to the natural serine cycle, the STC circumvents the emergence of the toxic pathway intermediate hydroxypyruvate and is harmonized to *E. coli*'s native metabolic set-up, avoiding the use of malyl-CoA synthetase and lyase which are absent in *E. coli*'s genome and could possibly interfere with the natural flux of metabolites through the TCA cycle when heterologously expressed. The STC is thus optimally suited for implementation in *E. coli* and other industrial relevant microbes with a similar central metabolism. Compared to other C<sub>1</sub>-assimilation routes, the autocatalytic STC shows the clear advantage of enabling formatotrophic growth at ambient CO<sub>2</sub> which allows a wider application spectrum and easier cultivation conditions. Furthermore, a recent theoretical analysis showed that serine cycle variants can support formatotrophic growth with high energetic efficiencies<sup>11</sup>. While in this study energy and carbon metabolism were coupled, the energy module of the STC could be replaced by using an efficient methanol dehydrogenase with methanol as an auxiliary energy and possible carbon source.

The results of this study clearly highlight the importance of ALE for achieving pathway activity. While rational engineering provides the genetic setup for novel pathways and might suffice to enable pathway activity in some cases, it can hardly address the genetic fine tuning which is often required to balance fluxes between native and non-native metabolic reactions. This seems especially true for metabolic engineering approaches that aim to achieve novel growth modes of the host<sup>4-6,8</sup>. In the case of the STC, ALE was used twice: first to enable cyclic pathway activity (ALE1, emergence of a  $\Delta$ 39bp deletion upstream of *thrABC*) and second to increase fluxes through the STC for achieving formatotrophic growth (ALE2, emergence of mutations in *thrA* and *pntAB*). Interestingly, only two evolutionary modifications can be directly linked to the pathway: (1) changes in the threonine synthesis operon, the only pathway module that was not rationally engineered in the strain and (2) changes in the expression of the membrane bound transhydrogenase. In contrast to what was observed for the engineering of natural autocatalytic C<sub>1</sub>-assimilation cycles (CBB<sup>4</sup> and RuMP<sup>6</sup>), no tuning of metabolic branch points seem to be required to allow full growth via the STC. Looking at the study from the "Design, Build, Test, Learn" perspective of synthetic biology<sup>32</sup> we can "learn" from these results that all pathway modules should have been overexpressed by engineering. Also, the transhydrogenase seems to be an important candidate gene for rational modifications, as the same mutation occurred independently in this and previous study<sup>5</sup>. Hence, future studies aiming to establish C<sub>1</sub>-assimilation routes requiring NADPH while using a NAD-dependent enzyme for energy generation should consider the overexpression of the transhydrogenase *ab initio*.

The results of this study clearly demonstrate the flexibility of *E. coli*'s central metabolic network and show for the first time that it is possible to introduce synthetic formate assimilation cycles in the heart of metabolism which enables robust formatotrophic growth. To create a platform strain for industrial applications, the formatotrophic strain created in this study could be combined with existing production modules to generate value-added chemicals from renewably produced formate<sup>33</sup>. This provides a new option to develop production processes based on microbial cell factories growing on CO<sub>2</sub>-derived C<sub>1</sub> substrates. Our study thus extends the solution space for designing processes based on CO<sub>2</sub>-derived feedstocks and points the way towards carbon negative chemical production in the framework of a circular economy.



## 274 **Acknowledgements**

275 The authors thank Lothar Willmitzer, Nico Claassens and Enrico Orsi for critical reading of the manuscript  
276 and helpful suggestions and Anne Michaelis for support with LC-MS measurements. SW thanks Caroline  
277 Gutjahr for guidance during the preparation of the manuscript. This work was funded by the Max Planck  
278 Society, by the German Ministry of Education and Research grant FormatPlant (part of BioEconomy 2030,  
279 Plant Breeding Research for the Bioeconomy), and MetAFor (031B0850B).

## 280 **Author contributions**

281 A.B.-E. designed and supervised the research;  
282 S.W. designed and conducted the experiments, analyzed the data and wrote the manuscript.  
283 S.W. and K.S. genetically engineered *E. coli* for growth on formate  
284 V.R. performed evolution experiments in Chi.Bio reactors, characterized isolated candidates and analyzed  
285 the experimental data  
286 H.H. performed flux balance analysis  
287 M.B. and V.D. designed and supervised evolution experiments  
288 S.N.L. performed initial experiments and assisted in writing the manuscript  
289

## 290 **Competing interests' statement**

291 The authors declare no competing interest  
292

## 293 **ORCID**

294 Sebastian Wenk: 0000-0001-9404-3535  
295 Vittorio Rainaldi: 0000-0003-3921-368X  
296 Hai He: 0000-0003-1223-2813  
297 Karin Schann: 0000-0003-1548-7643  
298 Madeleine Bouzon: 0000-0002-9581-6584  
299 Volker Döring: 0000-0002-9453-6572  
300 Steffen Lindner: 0000-0003-3226-3043  
301 Arren Bar-Even: 0000-0002-1039-4328  
302

## References

1. IPCC, 2022: Climate Change 2022: Impacts, Adaptation, and Vulnerability. Contribution of Working Group II to the Sixth Assessment Report of the Intergovernmental Panel on Climate Change [H.-O. Pörtner, D.C. Roberts, M. Tignor, E.S. Poloczanska, K. Mintenbeck, A. Alegría, M. Craig, S. Langsdorf, S. Lösschke, V. Möller, A. Okem, B. Rama (eds.)]. Cambridge University Press. In Press.
2. Bar-Even, A., Noor, E., Flamholz, A. & Milo, R. Design and analysis of metabolic pathways supporting formatotrophic growth for electricity-dependent cultivation of microbes. *Biochim. Biophys. Acta - Bioenerg.* **1827**, 1039–1047 (2013).
3. Satanowski, A. & Bar-Even, A. A one-carbon path for fixing CO<sub>2</sub>. *EMBO Rep.* **21**, 1–6 (2020).
4. Gleizer, S. *et al.* Conversion of *Escherichia coli* to generate all biomass carbon from CO<sub>2</sub>. *Cell* **179**, 1255-1263.e12 (2019).
5. Kim, S. *et al.* Growth of *E. coli* on formate and methanol via the reductive glycine pathway. *Nat. Chem. Biol.* **16**, 538–545 (2020).
6. Chen, F. Y. H., Jung, H. W., Tsuei, C. Y. & Liao, J. C. Converting *Escherichia coli* to a synthetic methyloph growing solely on methanol. *Cell* **182**, 933-946.e14 (2020).
7. Claassens, N. J. *et al.* Replacing the Calvin cycle with the reductive glycine pathway in *Cupriavidus necator*. *Metab. Eng.* **62**, 30–41 (2020).
8. Gassler, T. *et al.* The industrial yeast *Pichia pastoris* is converted from a heterotroph into an autotroph capable of growth on CO<sub>2</sub>. *Nat. Biotechnol.* **38**, 210–216 (2020).
9. Yishai, O., Lindner, S. N., Gonzalez de la Cruz, J., Tenenboim, H. & Bar-Even, A. The formate bio-economy. *Curr. Opin. Chem. Biol.* **35**, 1–9 (2016).
10. Claassens, N. J., Sánchez-Andrea, I., Sousa, D. Z. & Bar-Even, A. Towards sustainable feedstocks: A guide to electron donors for microbial carbon fixation. *Curr. Opin. Biotechnol.* **50**, 195–205 (2018).
11. Claassens, N. J., Cotton, C. A. R., Kopljar, D. & Bar-Even, A. Making quantitative sense of electromicrobial production. *Nat. Catal.* **2**, 437–447 (2019).
12. Cotton, C. A., Claassens, N. J., Benito-Vaquerizo, S. & Bar-Even, A. Renewable methanol and formate as microbial feedstocks. *Curr. Opin. Biotechnol.* **62**, 168–180 (2020).
13. Anthony, C. How half a century of research was required to understand bacterial growth on C<sub>1</sub> and C<sub>2</sub> compounds; the story of the serine cycle and the ethylmalonyl-CoA pathway. *Sci. Prog.* **94**, 109–137 (2011).
14. Sánchez-Andrea, I. *et al.* The reductive glycine pathway allows autotrophic growth of *Desulfovibrio desulfuricans*. *Nat. Commun.* **11**, 1–12 (2020).
15. Schuchmann, K. & Müller, V. Autotrophy at the thermodynamic limit of life: A model for energy conservation in acetogenic bacteria. *Nat. Rev. Microbiol.* **12**, 809–821 (2014).
16. Bowien, B. & Kusian, B. Genetics and control of CO<sub>2</sub> assimilation in the chemoautotroph *Ralstonia eutropha*. *Arch. Microbiol.* **178**, 85–93 (2002).
17. Bar-Even, A. Formate assimilation: The metabolic architecture of natural and synthetic pathways. *Biochemistry* **55**, 3851–3863 (2016).
18. Löwe, H. & Kremling, A. In-depth computational analysis of natural and artificial carbon fixation pathways. *BioDesign Res.* **2021**, 1–23 (2021).
19. Hordijk, W. Autocatalytic confusion clarified. *J. Theor. Biol.* **435**, 22–28 (2017).
20. Barenholz, U. *et al.* Design principles of autocatalytic cycles constrain enzyme kinetics and force low substrate saturation at flux branch points. *Elife* **6**, 1–32 (2017).
21. Sauer, U. & Eikmanns, B. J. The PEP-pyruvate-oxaloacetate node as the switch point for carbon flux distribution in bacteria. *FEMS Microbiol. Rev.* **29**, 765–794 (2005).

- 349 22. Keller, P. *et al.* Generation of an *Escherichia coli* strain growing on methanol via the ribulose  
350 monophosphate cycle. *Nat. Commun.* **13**, 5243 (2022).
- 351 23. Wu, C. *et al.* Acetyl-CoA synthesis through a bicyclic carbon-fixing pathway in gas-fermenting  
352 bacteria. *Nat. Synth.* **1**, 615–625 (2022).
- 353 24. Yu, H. & Liao, J. C. A modified serine cycle in *Escherichia coli* converts methanol and CO<sub>2</sub> to two-  
354 carbon compounds. *Nat. Commun.* **9**, (2018).
- 355 25. He, H., Höper, R., Dodenhöft, M., Marlière, P. & Bar-Even, A. An optimized methanol assimilation  
356 pathway relying on promiscuous formaldehyde-condensing aldolases in *E. coli*. *Metab. Eng.* **60**, 1–  
357 13 (2020).
- 358 26. Orsi, E., Claassens, N. J., Nickel, P. I. & Lindner, S. N. Growth-coupled selection of synthetic modules  
359 to accelerate cell factory development. *Nat. Commun.* **12**, 1–5 (2021).
- 360 27. Tishkov, V. I. & Popov, V. O. Catalytic mechanism and application of formate dehydrogenase.  
361 *Biochemistry (Moscow)* vol. 69 1252–1267 (2004).
- 362 28. Yishai, O., Bouzon, M., Döring, V. & Bar-Even, A. *In Vivo* assimilation of one-carbon via a synthetic  
363 reductive glycine pathway in *Escherichia coli*. *ACS Synth. Biol.* **7**, 2023–2028 (2018).
- 364 29. Flamholz, A., Noor, E., Bar-Even, A. & Milo, R. EQUilibrator - The biochemical thermodynamics  
365 calculator. *Nucleic Acids Res.* **40**, 770–775 (2012).
- 366 30. Steel, H., Habgood, R., Kelly, C. & Papachristodoulou, A. *In situ* characterisation and manipulation of  
367 biological systems with Chi.Bio. *PLoS Biol.* **18**, 1–12 (2020).
- 368 31. Lynn, S. P., Gardner, J. F. & Reznikoff, W. S. Attenuation regulation in the thr operon of *Escherichia*  
369 *coli* K-12: Molecular cloning and transcription of the controlling region. *Journal of Bacteriology* vol.  
370 152 (1982).
- 371 32. Nielsen, J. & Keasling, J. D. Engineering Cellular Metabolism. *Cell* **164**, 1185–1197 (2016).
- 372 33. Pontrelli, S. *et al.* *Escherichia coli* as a host for metabolic engineering. *Metab. Eng.* **50**, 16–46  
373 (2018).
- 374 34. Wenk, S., Yishai, O., Lindner, S. N. & Bar-Even, A. An engineering approach for rewiring microbial  
375 metabolism. *Methods in Enzymology* vol. 608 (Elsevier Inc., 2018).
- 376 35. Zelcbuch, L. *et al.* Spanning high-dimensional expression space using ribosome-binding site  
377 combinatorics. *Nucleic Acids Res.* **41**, (2013).
- 378 36. Barrick, J. E. *et al.* Identifying structural variation in haploid microbial genomes from short-read  
379 resequencing data using breseq. *BMC Genomics* **15**, 1–17 (2014).
- 380 37. Ebrahim, A., Lerman, J. A., Palsson, B. O. & Hyduke, D. R. COBRApy: COncstraints-Based  
381 Reconstruction and Analysis for Python. *BMC Syst. Biol.* **7**, (2013).
- 382 38. Monk, J.M., Lloyd, C.J., Brunk, E., Mih, N., Sastry, A., King, Z., Takeuchi, R., Nomura, W., Zhang, Z.,  
383 Mori, H., *et al.* iML1515, a knowledgebase that computes *Escherichia coli* traits. *Nat. Biotechnol.* **35**,  
384 (2017).
- 385 39. Bizouarn, T., Van Boxel, G. I., Bhakta, T. & Jackson, J. B. Nucleotide binding affinities of the intact  
386 proton-translocating transhydrogenase from *Escherichia coli*. *Biochim. Biophys. Acta - Bioenerg.*  
387 **1708**, 404–410 (2005).
- 388

## 389 **Methods**

### 390 **Chemicals and reagents**

391 Primers and oligonucleotides were synthesized by Integrated DNA Technologies (IDT). PCR reactions were carried out  
392 either using DreamTaq polymerase or Phusion High-Fidelity DNA Polymerase (Thermo Fisher Scientific). Restriction  
393 digests and ligations were performed using FastDigest enzymes and T4 DNA ligase (Thermo Fisher Scientific). Glycerol,  
394 sodium pyruvate, sodium acetate, glycine, sodium formate and sodium formate-<sup>13</sup>C were ordered from Sigma-Aldrich.

395

### 396 **Strains**

397 The *E. coli* strain SIJ488 was used for engineering purposes. *E. coli* strain DH5 $\alpha$  and *E. coli* strain ST18 were used for  
398 cloning and conjugation purposes. All strains used in this study are listed in Supplementary Table 1.

399

### 400 **Strain engineering**

401 Engineered strains were generated with recombineering techniques using SIJ488 as a base strain. For deletions, a  
402 linear dsDNA fragment containing an antibiotic resistance gene (kanamycin or chloramphenicol) was amplified with  
403 primers containing 50 bp homology arms flanking the target sequence to be deleted. The linear cassette was introduced  
404 into the strain via electroporation after induction of the recombination machinery with 15 mM arabinose for one hour.  
405 Colonies carrying the deletion were selected on LB plates supplemented with antibiotic. A similar procedure was used  
406 for genomic promoter exchange. To enable genomic overexpression of a synthetic operon, a conjugation-based genetic  
407 recombination method was used as described in<sup>34</sup>. In brief, the synthetic operon was cloned into a vector containing  
408 two 600bp homology regions compatible with the integration locus, chloramphenicol resistance gene (*cam*<sup>R</sup>), a  
409 levansucrase gene (*sacB*), and the conjugation gene *traJ* for the transfer of the plasmid. The resulting plasmid was  
410 transformed into chemically competent *E. coli* ST18 strains. Positive clones growing on chloramphenicol medium  
411 supplemented with 5-aminolevulinic acid (50  $\mu$ g ml<sup>-1</sup>) were identified by colony PCR, and the confirmed recombinant  
412 ST18 strain was used as donor strain for the conjugation. Chloramphenicol resisting recipient *E. coli* strains were  
413 screened as positive strains for the first round of recombination. Subsequently, sucrose counter selection and kanamycin  
414 resistance tests were carried out to isolate recombinant *E. coli* strains with the correct synthetic operon integration into  
415 chromosome. All constructs were verified via PCR and sequencing.

416

### 417 **Synthetic-Operon construction**

418 Before cloning the genes into synthetic operons, each gene was codon optimized for *E. coli* K-12 and an N-terminal  
419 6xHis-tag was added. All genes were inserted into a cloning vector that attached a synthetic ribosome binding site  
420 upstream of the gene<sup>35</sup>. The same entry vector was then used for stepwise assembly of multi gene operons as described  
421 in<sup>34</sup>. Plasmids were constructed via restriction and ligation using standard kits and protocols supplied by Thermo Fischer  
422 Scientific. The assembled construct was then transferred to an expression vector containing a promoter and terminator  
423 sequence<sup>34</sup>.

424

### 425 **Growth media**

426 Cloning and engineering steps were performed using Lysogeny Broth medium (10 g/l tryptone, 10 g/l NaCl, 5 g/l yeast  
427 extract + 15 g/l agar for plates) with the appropriate amount of relevant antibiotics (ampicillin/carbenicillin (100  $\mu$ g/ml),  
428 kanamycin (50  $\mu$ g/ml), chloramphenicol (30  $\mu$ g/ml) and/or streptomycin (50  $\mu$ g/ml)). Engineered and evolved strains  
429 were grown either in M9 minimal medium (50 mM Na<sub>2</sub>HPO<sub>4</sub>, 20 mM KH<sub>2</sub>PO<sub>4</sub>, 1 mM NaCl, 20 mM NH<sub>4</sub>Cl, 2 mM MgSO<sub>4</sub>,  
430 and 100  $\mu$ M CaCl<sub>2</sub>) or HEPES minimal medium (HMM, 200 mM HEPES, 1.32 mM K<sub>2</sub>HPO<sub>4</sub>, 0.5% NaCl, 1% NH<sub>4</sub>Cl, 2  
431 mM MgSO<sub>4</sub>, and 100  $\mu$ M CaCl<sub>2</sub>) supplemented with trace elements (50 mg/L EDTA, 31 mM FeCl<sub>3</sub>, 6.2 mM ZnCl<sub>2</sub>, 0.76  
432 mM CuCl<sub>2</sub>·2H<sub>2</sub>O, 0.42 mM CoCl<sub>2</sub>·6H<sub>2</sub>O, 1.62 mM H<sub>3</sub>BO<sub>3</sub>, 81nM MnCl<sub>2</sub>·4H<sub>2</sub>O) and the relevant carbon sources.

433

## Growth experiments

434

435

436

437

438

439

440

441

442

443

444

445

446

447

448

## Tube evolution (ALE1)

449

450

451

452

453

454

455

456

457

458

459

460

## Turbidostat evolution experiment (ALE2)

461

462

463

464

465

466

467

468

469

470

## <sup>13</sup>C labeling experiment

471

472

473

474

475

476

## Sample preparation for LC-MS analysis

477

478

479

480

481

482

483

484

485

486

487

## Whole-genome sequencing

488

489

490

491

Genomic DNA was extracted using a commercial kit (Mackerey Nagel) starting from 2-4 ml of overnight culture in LB. A minimum of 300 ng was sent for sequencing to NovoGene. Results were analyzed using the open source breseq software<sup>36</sup>. All NGS data was deposited at the Genome Sequence Archive.



491  
492  
493  
494  
495  
496  
497  
498  
499  
500  
501  
502  
503  
504  
505  
506  
507  
508  
509  
510  
511  
512  
513  
514

## Flux balance analysis

Flux balance analysis (FBA) was used for comparing formate dependency of the STC under formate only or formate-glycine conditions. The modeling was conducted with COBRApy<sup>37</sup> using the most updated *E. coli* genome-scale metabolic model *ML1515*<sup>38</sup> with curations and changes: (i) transhydrogenase (THD2pp) translocates one proton instead of two<sup>39</sup>; (ii) homoserine dehydrogenase (HSDy) was set to irreversibly produce homoserine<sup>25</sup>; (iii) anaerobic relevant reactions, PFL, OBTFL, FDR2, and FDR3, were removed from the model; (iv) POR5, GLYCK, FDH4pp, FDH5pp, GART, DRPA, PAI2T, G6PDH2r, and ETHAAL were also knocked out to block unrealistic routes; (v) formate dehydrogenase (FDH) and pyruvate carboxylase (PYC) were implemented in the model; (vi) gene knock outs of the XGAS\_C1 strain, i.e. *gcvTHF*, *aceE*, *poxB*, *serA* and additional *aceA* in the case of formate and glycine feeding condition, were also introduced in the model. We further fixed the upper and lower bounds of the biomass reaction and change the objective function to formate uptake (EX\_for\_e) to find the flux distribution resulting in biomass flux of the fixed value at the lowest possible flux through formate uptake, using formate only or formate and glycine as carbon sources. We expressed the formate dependency as the slope of biomass reaction, i.e. growth rate, and formate uptake rate from the modeling. The full code, including the changes described above, was deposited at <https://github.com/he-hai/PubSuppl>, within "2022\_STC" the directory.

## Data availability

Additional information on the experimental setup as well as detailed results are available from the corresponding author upon request. Any strains and plasmids generated during this study are available upon completing a Materials Transfer Agreement.

## Code availability

MATLAB and breseq codes used for the analysis of the experiments are available from the corresponding author upon request.